

Phospholipid Flippase ATP10A Translocates Phosphatidylcholine and Is Involved in Plasma Membrane Dynamics*

Received for publication, March 29, 2015, and in revised form, May 1, 2015. Published, JBC Papers in Press, May 6, 2015, DOI 10.1074/jbc.M115.655191

Tomoki Naito^{†1}, Hiroyuki Takatsu^{†1}, Rie Miyano[‡], Naoto Takada[§], Kazuhisa Nakayama[‡], and Hye-Won Shin^{‡2}

From the [†]Graduate School and the [§]Faculty of Pharmaceutical Sciences, Kyoto University, Sakyo-ku, Kyoto 606-8501, Japan

Background: The enzymatic activities of the ATP10 family of mammalian P4-ATPases are unknown.

Results: ATP10A catalyzes the flipping of NBD-PC and expression of ATP10A altered cell shape and inhibited cell adhesion and spreading.

Conclusion: The enhanced PC flipping activity by ATP10A changes the lipid composition, which may cause a delay in cell spreading.

Significance: This is the first evidence showing that PC flipping activity by P4-ATPase is associated with the plasma membrane dynamics.

We showed previously that ATP11A and ATP11C have flippase activity toward aminophospholipids (phosphatidylserine (PS) and phosphatidylethanolamine (PE)) and ATP8B1 and that ATP8B2 have flippase activity toward phosphatidylcholine (PC) (Takatsu, H., Tanaka, G., Segawa, K., Suzuki, J., Nagata, S., Nakayama, K., and Shin, H. W. (2014) *J. Biol. Chem.* 289, 33543–33556). Here, we show that the localization of class 5 P4-ATPases to the plasma membrane (ATP10A and ATP10D) and late endosomes (ATP10B) requires an interaction with CDC50A. Moreover, exogenous expression of ATP10A, but not its ATPase-deficient mutant ATP10A(E203Q), dramatically increased PC flipping but not flipping of PS or PE. Depletion of CDC50A caused ATP10A to be retained at the endoplasmic reticulum instead of being delivered to the plasma membrane and abrogated the increased PC flipping activity observed by expression of ATP10A. These results demonstrate that ATP10A is delivered to the plasma membrane via its interaction with CDC50A and, specifically, flips PC at the plasma membrane. Importantly, expression of ATP10A, but not ATP10A(E203Q), dramatically altered the cell shape and decreased cell size. In addition, expression of ATP10A, but not ATP10A(E203Q), delayed cell adhesion and cell spreading onto the extracellular matrix. These results suggest that enhanced PC flipping activity due to exogenous ATP10A expression alters the lipid composition at the plasma membrane, which may in turn cause a delay in cell spreading and a change in cell morphology.

In eukaryotic cells, the lipid bilayer of the plasma membrane and organelle membranes exhibits asymmetric lipid distributions (1–3). For example, in human erythrocytes, phosphatidyl-

serine (PS)³ and phosphatidylethanolamine (PE) are restricted primarily to the inner leaflet of the plasma membrane, whereas phosphatidylcholine (PC) and sphingomyelin (SM) are exposed on the cell surface (4, 5).

An ATP-dependent aminophospholipid translocase activity was discovered in the plasma membrane of human erythrocytes by Seigneuret and Devaux (6). Subsequently, P4-ATPases were identified as flippases in eukaryotic membranes (7–11). The yeast P4-ATPases (phospholipid flippases), Drs2p and Dnf1p/Dnf2p, flip PS and PC/PE, respectively (9, 12). Mammals express 14 P4-ATPases: class 1 (ATP8A1, ATP8A2, ATP8B1, ATP8B2, ATP8B3, and ATP8B4), class 2 (ATP9A and ATP9B), class 5 (ATP10A, ATP10B, and ATP10D), and class 6 (ATP11A, ATP11B, and ATP11C). These P4-ATPases form heteromeric complexes with members of the CDC50 family (10, 13). We and others have shown that most of the 14 mammalian P4-ATPases, except for ATP9A and ATP9B, require association with CDC50 for their exit from the endoplasmic reticulum (ER) and subsequent subcellular localization (14–18). Moreover, we recently showed that ATP11A and ATP11C can flip NBD-labeled aminophospholipids NBD-PS and -PE and that ATP8B1 and ATP8B2 preferentially flip NBD-PC at the plasma membrane (19).

The phospholipid asymmetry regulated by P4-ATPases is indispensable for the homeostasis of multicellular organisms. Loss of phospholipid asymmetry due to mutations in the human FIC1/ATP8B1 (a member of the P4-ATPase family) gene causes progressive familial intrahepatic cholestasis (PFIC) (20, 21). We showed that some ATP8B1 mutants found in type 1 progressive familial intrahepatic cholestasis fail to flip PC, indicating that PC flipping activity at the bile canaliculi is critical for proper bile excretion in liver (19). ATP8A1 deficiency

* This work was supported in part by grants from the Ministry of Education, Culture, Sports, Science, and Technology of Japan and by the Takeda Science Foundation.

¹ Both authors contributed equally to this work.

² To whom correspondence should be addressed: Graduate School of Pharmaceutical Sciences, Kyoto University, Sakyo-ku, Kyoto 606-8501, Japan. Tel: 81-75-753-4537; Fax 81-75-753-4557; E-mail: shin@pharm.kyoto-u.ac.jp.

³ The abbreviations used are: PS, phosphatidylserine; PE, phosphatidylethanolamine; PC, phosphatidylcholine; P4-ATPase, type IV P-type ATPase; NBD, nitrobenzoxadiazole; SM, sphingomyelin; ER, endoplasmic reticulum; HBSS, Hanks' balanced salt solution; DSP, dithiobis[succinimidylpropionate]; PIP₂, phosphatidylinositol 4,5-bisphosphate; TfR, transferrin receptor.

causes surface externalization of PS in the hippocampus and delays hippocampus-dependent learning (22). ATP11C deficiency causes a defect in B-cell maturation, altered erythrocyte shape, and anemia (23, 24). During apoptosis, ATP11C undergoes caspase-mediated cleavage and is consequently inactivated, resulting in PS exposure on the cell surface (25). Heterozygous deletion of ATP10A in mice causes diet-induced obesity, type 2 diabetes, and nonalcoholic fatty liver disease, implicating ATP10A in obesity-related metabolic abnormalities (26). ATP10A is also implicated in regulation of insulin-stimulated glucose uptake (27, 28). However, the flippase activity and substrate specificities of ATP10A remain to be determined.

In this study, we characterized the interaction of the class 5 P₄-ATPases (ATP10A, ATP10B, and ATP10D) with CDC50 proteins and investigated their flippase activities. We found that class 5 P₄-ATPases preferentially interact with CDC50A. Importantly, plasma membrane-localized ATP10A exhibited flippase activity toward NBD-PC. Moreover, elevated PC flipping activity due to exogenous ATP10A expression caused changes in cell shape and cell size, and inhibited cell adhesion and spreading onto the extracellular matrix.

Experimental Procedures

RT-PCR—Total RNA from HeLa cells, isolated using the RNeasy Mini Kit (Qiagen) or Isogen (Nippon Gene), was then subjected to RT-PCR analysis using the SuperScript III One-Step RT-PCR system (Invitrogen). The CDC50A cDNA was amplified using the following primer pair: sense, GAAAAAG-AAAGGTATTGCTTGGTG, and antisense, GTAATGTCA-GCTGTATTACTACTG.

Plasmids—Expression Vectors for C-terminally HA-tagged P₄-ATPases and N-terminally FLAG-tagged CDC50A or CDC50B were constructed as described previously (18). ABCB4 cDNA was a kind gift from Kazumitsu Ueda (Kyoto University). The pCAG-based vector for expression of ABCB4 with a C-terminal HA tag was constructed. ABCB4 cDNA was cloned into the pENTR3C vector (Invitrogen), and the pCAG-HA-based vector was prepared as described previously (18). Transfer of the ABCB4 cDNA to expression vectors was performed using the Gateway system (Invitrogen).

Antibodies and Reagents—The sources of antibodies used in the present study were as follows: monoclonal mouse anti-transferrin receptor (TfnR, H68.4) was from Zymed Laboratories Inc.; monoclonal mouse anti-calnexin, anti-EEA1, and anti-Lamp-1 from BD Biosciences; monoclonal rat anti-HA (3F10) from Roche Applied Science; polyclonal rabbit anti-FLAG from Sigma-Aldrich; monoclonal mouse anti-DYKD-DDK (1E6) from Wako Chemicals; mouse anti- β -tubulin from Millipore; Alexa Fluor 488-conjugated monoclonal mouse anti-CD147 (HIM6) from BioLegend; Alexa Fluor-conjugated secondary antibodies from Molecular Probes; and Cy3-conjugated and horseradish peroxidase-conjugated secondary antibodies from Jackson ImmunoResearch Laboratories. For monoclonal mouse antibody to MHCI, a hybridoma clone (W6/32) was purchased from ATCC, Alexa Fluor 488-conjugated phalloidin from Molecular Probes, and fibronectin from Sigma. The NBD-labeled phospholipids (Avanti Polar Lipids) used were NBD-PS

(1-oleoyl-2-[6-[(7-nitro-2-1,3-benzoxadiazol-4-yl)amino]hexanoyl]-sn-glycero-3-phosphoserine), NBD-PE (1-oleoyl-2-[6-[(7-nitro-2-1,3-benzoxadiazol-4-yl)amino]hexanoyl]-sn-glycero-3-phosphoethanolamine), NBD-PC (1-oleoyl-2-[6-[(7-nitro-2-1,3-benzoxadiazol-4-yl)amino]hexanoyl]-sn-glycero-3-phosphocholine), and NBD-SM (*N*-[6-[(7-nitro-2-1,3-benzoxadiazol-4-yl)amino]hexanoyl]-sphingosine-1-phosphocholine).

Cell Culture, siRNA-mediated Knockdown, and Immunofluorescence Analysis—HeLa cells were maintained in Eagle's minimum essential medium (Nacalai Tesque, Inc.) supplemented with 5 or 10% heat-inactivated fetal bovine serum (Invitrogen) and non-essential amino acids (Nacalai Tesque). Preparation of pools of siRNAs for CDC50A and ATP10A and knockdowns using these siRNA pools were performed as described previously (18, 29). Briefly, a pool of siRNAs directed against nucleotides 597–1086 of CDC50A mRNA or nucleotides 655–1399 of ATP10A mRNA (the A residue of the initiation Met codon was defined as nucleotide 1) was prepared using the BLOCK-iT RNAi TOPO transcription kit and BLOCK-iT Dicer RNAi kit (Invitrogen). HeLa cells were transfected with the siRNA pool using Lipofectamine 2000 (Invitrogen) and incubated for 24 h. The transfected cells were then transferred to a culture dish containing coverslips, incubated for an additional 48 h, and processed for immunoblotting, immunofluorescence, and RT-PCR analyses.

For retroviral production, pMXs-neo-derived vectors for expression of HA-tagged P₄-ATPases were co-transfected with pEF-gag-pol and pCMV-VSVG-Rsv-Rev into HEK293T cells as described previously (18). The resultant retroviruses were concentrated and then used to infect HeLa cells to establish stable cell lines. The infected cells were selected in medium containing G418 (1 mg/ml). To transiently express P₄-ATPases, HeLa cells were transfected with a pCAG-HA-based vector carrying P₄-ATPase cDNA and a pcDNA3-FLAG-based vector carrying CDC50A cDNA (18) using X-tremeGENE 9 (Roche Applied Science) or polyethyleneimine (Sigma). Two days later, the transfected cells were fixed for immunofluorescence or lysed for immunoblotting analysis.

Immunofluorescence staining was performed as described previously (30, 31) and visualized using an Axiovert 200MAT microscope (Carl Zeiss, Thornwood, NY). For the plasma membrane staining, cells were incubated with Alexa Fluor 488-conjugated anti-CD147 or anti-MHCI antibody for 10 min at room temperature prior to permeabilization, fixed, and processed for immunofluorescence analysis. To obtain quantitative data of cellular areas, the surface areas of cells were stained with anti-MHCI antibody, and CDC50A- or P₄-ATPases-expressing cells were chosen. The areas of the cells were measured with ImageJ software.

Flippase Assay—Incorporation of NBD-phospholipids was analyzed by flow cytometry as described previously (19). HeLa cells were detached from dishes in PBS containing 5 mM EDTA and then harvested by centrifugation. The cells (1×10^6 cells/sample) were washed and equilibrated at 15 °C for 15 min in 500 μ l of Hanks' balanced salt solution (pH 7.4) containing 1 g/liter glucose (HBSS-glucose). An equal volume of 2 μ M NBD-phospholipid in HBSS-glucose was added to the cell suspension and incubated at 15 °C. At each time point, 200 μ l of cell suspension

ATP10A Translocates Phosphatidylcholine

was collected and mixed with 200 μ l of ice-cold HBSS-glucose containing 5% fatty acid-free BSA (Wako Pure Chemicals) in order to extract NBD-lipids incorporated into the exoplasmic leaflet of the plasma membrane, as well as unincorporated ones. Next, 5,000 or 10,000 cells were analyzed with a FACSCalibur flow cytometer (BD Biosciences) to measure fluorescence of NBD-lipids translocated into the cytoplasmic leaflet of the plasma membrane, and the mean fluorescence intensity per cell was calculated. Propidium iodide-positive cells (*i.e.* dead cells) were excluded from the analysis.

Immunoprecipitation—HeLa cells were transfected using polyethyleneimine with different combinations of expression vectors for P4-ATPase and CDC50 and grown for 2 days. The cells were then lysed in lysis buffer (20 mM HEPES (pH 7.4), 150 mM NaCl, 1 mM EDTA, and 1% Nonidet P-40) containing a protease inhibitor mixture (Nacalai Tesque) at 4 °C for 30 min. The lysates were centrifuged at maximum speed for 20 min at 4 °C in a microcentrifuge to remove cellular debris and insoluble materials. The supernatant was incubated with an anti-HA antibody at 4 °C for 15 min and then incubated with protein G-coupled Dynabeads (Invitrogen) at 4 °C overnight. After washing, the beads were incubated in SDS sample buffer including β -mercaptoethanol at 37 °C for 2 h, and the supernatant was subjected to SDS-PAGE and immunoblot analysis using rat anti-HA, mouse anti-DYKDDDK, or mouse anti- β -tubulin antibody. Immunoblots were developed using a Chemi-Lumi One L or Chemi-Lumi One Super kit (Nacalai Tesque), recorded on a LAS-3000 bioimaging system (Fujifilm), and quantified using Image Gauge software (version 4.0, Fujifilm).

For cross-linker treatment, 10 mM (dithiobis[succinimidylpropionate]) (DSP, Thermo Scientific) was freshly prepared by dissolving in dimethyl sulfoxide. Transfected cells were washed twice with PBS++ (including 0.1 mM CaCl₂ and 0.1 mM MgCl₂) and treated with 1 mM DSP in PBS++ for 30 min at room temperature. To stop the reaction, 1 M Tris (pH 7.5) was added at a final concentration of 20 mM and incubated for 15 min at room temperature. The cells were washed with PBS(–), lysed, and immunoprecipitated as described above.

Cell Adhesion and Spreading Assay—HeLa cells were detached from dishes in PBS containing 5 mM EDTA and harvested by centrifugation. The cells were washed and resuspended in complete growth medium, plated onto 24-well plates (1 \times 10⁵ cells/well), and incubated at 37 °C in 5% CO₂ for the indicated times. The same number of cells was removed, and DNA content was measured using a Qubit fluorometer (Life Technologies). After incubation at 37 °C, the cells were fixed with 96% of ethanol and stained with 1% crystal violet in 10% ethanol at room temperature. After the cells were washed with PBS, the stain was extracted using 1% Triton X-100 and processed to measure absorbance at 570 nm. Absorbance was normalized to the ratio of DNA content.

For the cell spreading assay, cells were harvested as described above, washed with serum-free Eagle's minimum essential medium, and seeded onto fibronectin- or FBS-coated coverslips. After incubation at 37 °C in 5% CO₂ for the indicated times, cells were fixed with 3% paraformaldehyde and subjected to immunofluorescence analysis. Alexa Fluor 488-conjugated

phalloidin was added during incubation with secondary antibody. Immunofluorescence staining was performed as described previously (30, 31) and observed using an Axiovert 200MAT microscope (Carl Zeiss). To obtain quantitative data on the extent of cell spreading, cells were stained with phalloidin, and randomly chosen fields were acquired. Cell areas were measured using MetaMorph software (Molecular Devices).

Results

CDC50-dependent Subcellular Localization of ATP10A, ATP10B, and ATP10D—Previously, we demonstrated that CDC50 is required for proper subcellular localization of human P4-ATPases and performed a co-immunoprecipitation analysis that elucidated its physical interactions with P4-ATPases (18), with the exception of the class 5 P4-ATPases (ATP10A, ATP10B, and ATP10D). In this study, we transiently expressed C-terminally HA-tagged class 5 P4-ATPases in HeLa cells, either alone or in combination with N-terminally FLAG-tagged CDC50A or CDC50B (Fig. 1, A–C), and observed their localization (Fig. 1; *insets* (left panels in A–F) show CDC50 expression). In the absence of exogenous CDC50 expression or in the presence of exogenous CDC50B, all three class 5 P4-ATPases were predominantly localized to the ER, as demonstrated by their almost complete overlap with an ER marker protein, calnexin (Fig. 1, A–C, *a-a'* and *c-c'*). By contrast, in the presence of exogenous CDC50A, ATP10A and ATP10D were localized primarily on the plasma membrane (Fig. 1, *Ab* and *Cb*), and ATP10B was localized on punctate structures in the cytoplasm (Fig. 1*Bb*) as described previously (18). The perinuclear staining of ATP10A, ATP10B, and ATP10D might reflect protein *en route* to the plasma membrane during biosynthetic pathway. Next we compared the subcellular localization of these ATPases with organelle marker proteins (Fig. 1, *D* and *E*). ATP10A and ATP10D were colocalized extensively with a plasma membrane marker, CD147 (Fig. 1*D*). On the other hand, the punctate ATP10B staining overlapped with that of a late endosomal/lysosomal marker, Lamp-1 (Fig. 1*E*), but only rarely with an early endosomal marker, EEA1, or an early/recycling endosomal marker, TfnR, indicating that ATP10B is localized mainly to late endosomes and lysosomes. In the presence of CDC50A, ATPase-deficient glutamate-to-glutamine mutants (19, 32) of ATP10A and ATP10D were colocalized with markers for the plasma membrane, whereas an analogous mutant of ATP10B was localized to endosomes/lysosomes (Fig. 1*F*) indicating that ATPase activity may not be a prerequisite for their exit from the ER or delivery to their final destinations. Notably, expression of ATP10A, but not ATP10A-(E203Q), caused significant changes in cell shape (Fig. 1, *Ab*, *D*, and *F*); we discuss the physiological relevance of this observation below.

Association of ATP10A, ATP10B, and ATP10D with CDC50A—We next investigated whether ATP10A, ATP10B, and ATP10D interact physically with CDC50A. To this end, we transiently transfected HeLa cells with expression vectors for C-terminally HA-tagged P4-ATPase and FLAG-CDC50A, prepared total lysates from the transfected cells, immunoprecipitated the lysates with anti-HA antibody, and subjected the immunoprecipitates to immunoblotting with anti-HA or anti-FLAG anti-

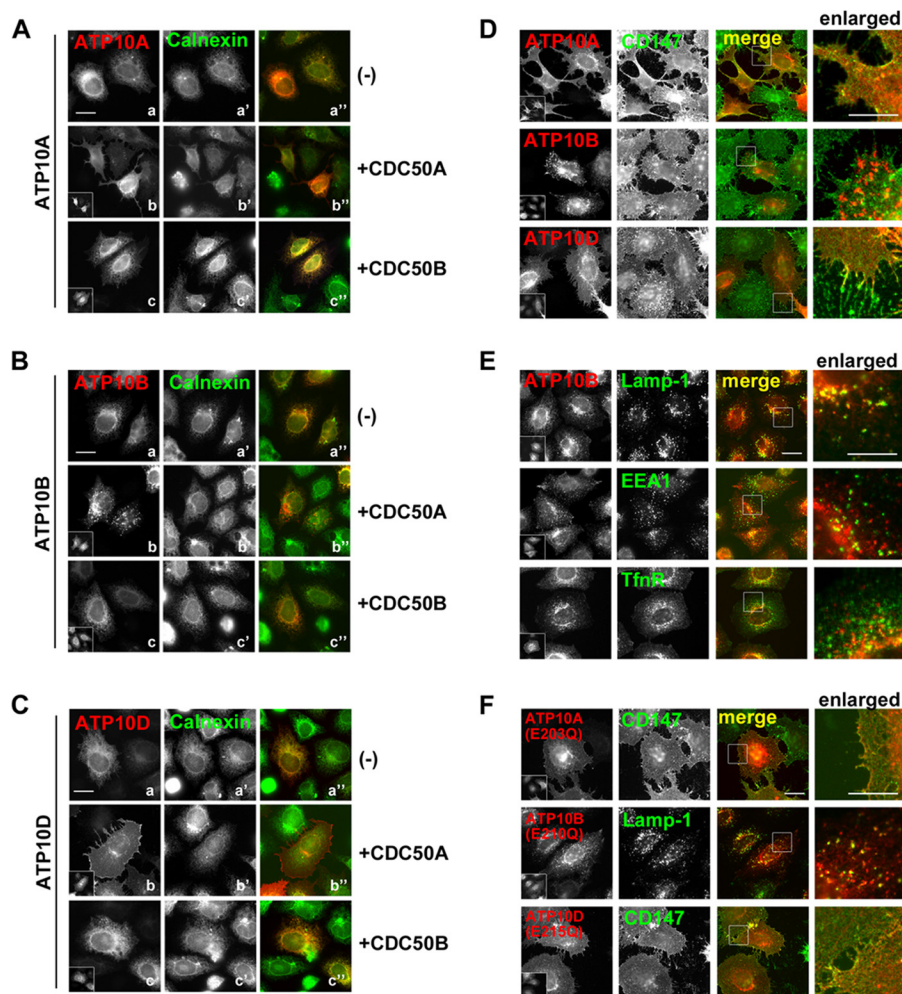


FIGURE 1. Changes in localization of transiently expressed P4-ATPases upon co-expression of CDC50. HeLa cells were transiently co-transfected with an expression vector for C-terminally HA-tagged P4-ATPase and a control pcDNA3 vector (A–C, *a* and *a'*) or an expression vector for N-terminally FLAG-tagged CDC50A (A–C, *b* and *b'*, *D*, and *E*) or CDC50B (A–C, *c* and *c'*). In *F*, HeLa cells were transiently co-transfected with an expression vector for a glutamate mutant of P4-ATPase with a C-terminal HA tag and FLAG-CDC50A. After 48 h of transfection, the cells were fixed and processed for immunofluorescence microscopy. A–C, cells were stained with anti-HA, anti-FLAG, and anti-calnexin antibodies followed by Cy3-conjugated anti-rat, Alexa Fluor 647-conjugated anti-rabbit, and Alexa Fluor 488-conjugated anti-mouse antibodies. *D* and *F*, for plasma membrane staining, cells were incubated with Alexa Fluor 488-conjugated anti-CD147 antibody to label the surface prior to permeabilization. After permeabilization, cells were incubated with anti-HA and anti-FLAG antibodies followed by Cy3-conjugated anti-rat and Alexa Fluor 647-conjugated anti-rabbit antibodies. *E* and *F*, cells were fixed and stained with antibodies against HA or FLAG and Lamp-1, EEA1, or TfnR, as indicated, followed by Cy3-conjugated anti-rat, Alexa Fluor 647-conjugated anti-rabbit, and Alexa Fluor 488-conjugated anti-mouse antibodies. *Insets* show cells expressing FLAG-tagged CDC50A or CDC50B. *Bars*, 20 μm . *Bars in enlarged images*, 10 μm .

body (Fig. 2). Expression of the tagged proteins was confirmed by immunoblotting of total cell lysates (Fig. 2, *Input panels*). As shown in the *bottom two panels* in Fig. 2A, ATP10A-HA co-immunoprecipitated FLAG-CDC50A (*lane 3*) but much less efficiently than ATP8B1 and ATP11A (*lanes 6 and 7*); FLAG-CDC50A migrated as a smear in the SDS-polyacrylamide gel, probably due to heterogeneous glycosylation (18). To our surprise, however, FLAG-CDC50A was not co-immunoprecipitated when co-expressed with ATP10B-HA or ATP10D-HA (Fig. 2A, *lanes 4 and 5*). These results suggest that the interaction of the ATP10 proteins with CDC50A might be transient or much weaker than those of other P4-ATPases. To overcome this problem, we performed co-immunoprecipitation after treating the cells with a thiol-cleavable cross-linker, DSP (Fig. 2B). The transfected cells were treated with DSP, and after quenching, they were lysed, immunoprecipitated with anti-HA antibody, and subjected to SDS-PAGE

under reducing conditions followed by immunoblotting with anti-HA or anti-FLAG antibody (Fig. 2B). By the DSP treatment, CDC50A was co-immunoprecipitated with ATP10B and ATP10D (Fig. 2B, *lanes 12 and 13*) as well as with ATP10A (*lane 11*). The amount of CDC50A that co-immunoprecipitated with ATP10D increased dramatically in the presence of DSP (Fig. 2, compare *lane 5* with *lane 13*), and the amount that co-immunoprecipitated with ATP10A or ATP10B increased slightly (compare *lanes 3 and 11* or *lanes 4 and 12*, respectively). Thus, the interaction between CDC50A and ATP10 proteins, especially ATP10B and ATP10D, may not be as stable as the interaction between CDC50A and other P4-ATPases such as ATP8B1 and ATP11A. Because nonspecific bands can be detected in the presence of DSP (Fig. 2B, *lanes 9 and 10*), we made use of a transmembrane protein, ABCB4, an ABC transporter that localizes to the plasma membrane (33), as a negative control

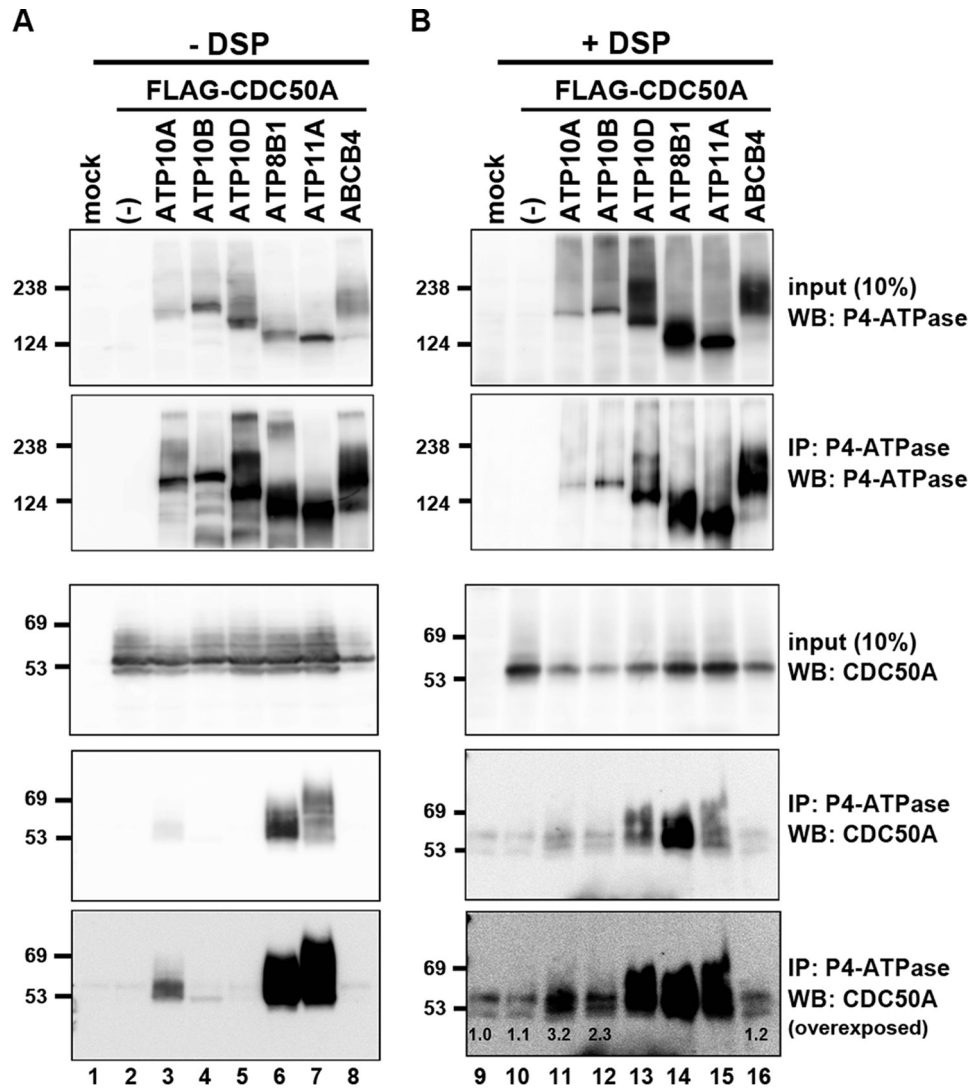


FIGURE 2. Co-immunoprecipitation analysis of interactions between P4-ATPases and CDC50 proteins. HeLa cells were transfected with an expression vector for FLAG-CDC50A, either alone (*lanes 2 and 10*) or in combination with an expression vector for HA-tagged P4-ATPase or HA-tagged ABCB4 (*lanes 8 and 16*). In *mock* lanes (*lanes 1 and 9*), HeLa cells were transfected with an empty vector in the absence (*A*) or presence (*B*) of cross-linker DSP as indicated. After 48 h of transfection, the cells were mock-treated with dimethyl sulfoxide (*A*) or the cross-linker DSP (*B*), lysed, and immunoprecipitated with anti-HA antibody. Bound material and 10% of input were subjected to SDS-PAGE and immunoblotting using anti-HA or anti-DYKDDDK antibody. The numerical values shown in the *bottom panel* of *B* are the relative band intensities of co-immunoprecipitated CDC50A when the band intensity in the *mock* lane is expressed as 1.0.

(*lane 16*) and quantified the band intensities (Fig. 2*B*, *bottom panel*). Taken together, these data indicate that CDC50A interacts physically with ATP10 proteins, but with lower affinity than with other P4-ATPases, and is required for exit from the ER followed by localization to their destinations.

ATP10A Translocates NBD-PC—In a recent study, we elucidated the flippase activities and substrate specificities of plasma membrane-localizing P4-ATPases ATP8B1, ATP8B2, ATP11A, and ATP11C using NBD-labeled phospholipids (19). ATP11A translocates aminophospholipids (PS and PE) (Fig. 3, *B* and *C*), whereas ATP8B1 preferentially flips PC (Fig. 3*A*) (19). Here, we investigated the flippase activities of ATP10A and ATP10D, which are also localized to the plasma membrane (see Fig. 1). To this end, we first established cells stably expressing ATP10A, ATP10A(E203Q), or ATP10D by infection with recombinant retrovirus. Although exogenous expression of CDC50A is required for the proper localization of transiently expressed ATP10 protein (see Fig. 1), stably expressed ATP10A and

ATP10D were detected at the plasma membrane in the absence of exogenous CDC50A expression (see Fig. 5*A*, *a*, *a'*, *b*, *b'*, *e*, and *e'*). As described previously (19), this probably reflects the fact that the endogenous level of CDC50A is sufficient for localization of ATP10A and ATP10D expressed at moderate levels in stable cells. Intriguingly, cells stably expressing ATP10A exhibited a highly selective flippase activity toward NBD-PC (Fig. 3, *A* and *E*) but not toward any other NBD-lipids that we examined (Fig. 3, *B–D* and *F–H*). Furthermore, the PC flipping activity of ATP10A-expressing cells was much higher than that of cells stably expressing ATP8B1 (Fig. 3*A*). By contrast, cells stably expressing ATP10A(E203Q), an ATPase-deficient mutant, did not exhibit significant flippase activity toward NBD-PC (Fig. 3*A*), although the expression level of ATP10A(E203Q) was comparable with that of ATP10A (Fig. 3*I*), indicating that the increase in translocation of NBD-PC from the exoplasmic to the cytoplasmic leaflet in ATP10A-expressing cells was dependent on the ATPase cycle of ATP10A.

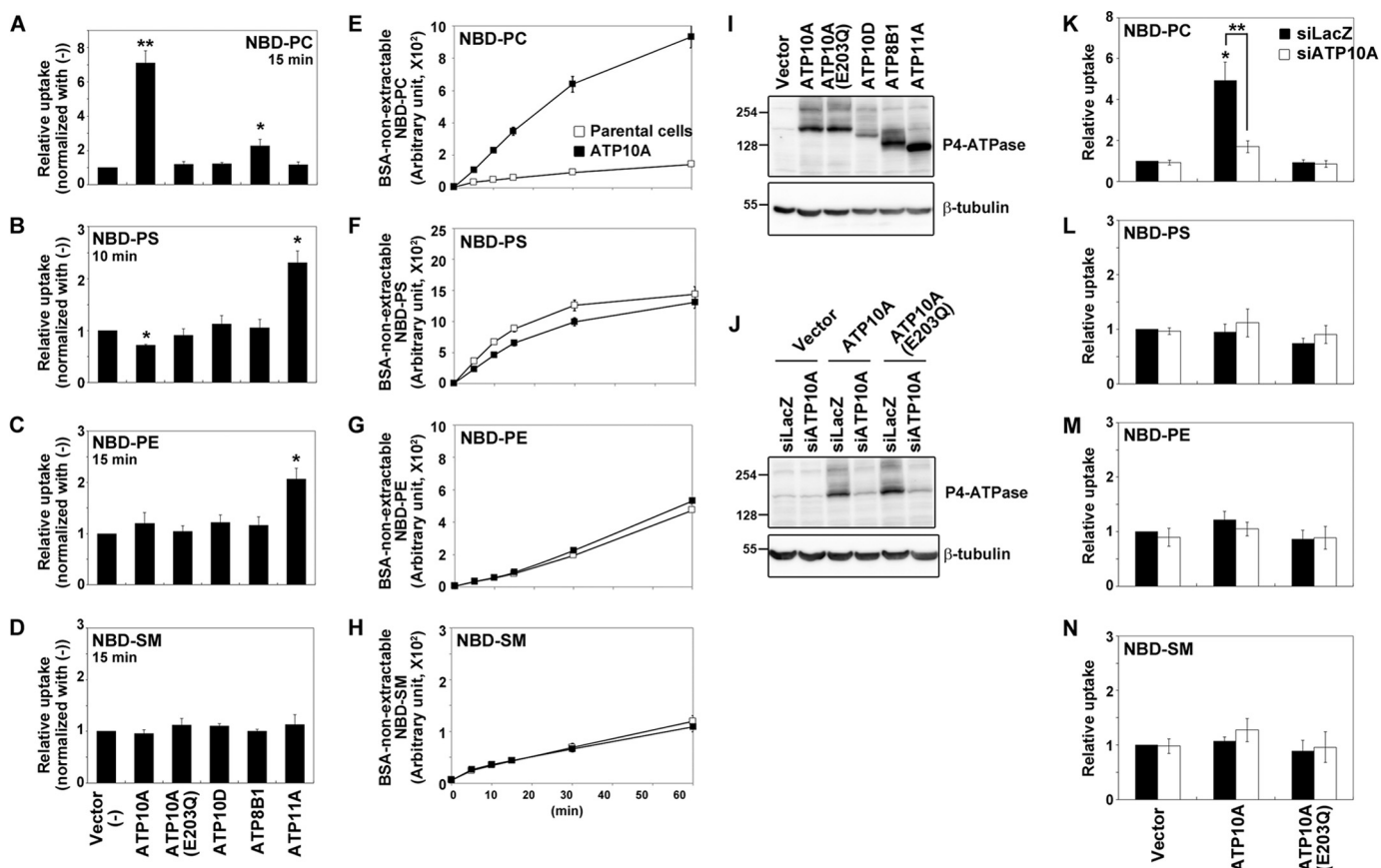


FIGURE 3. Flippase activities across the lipid bilayer of the plasma membrane in HeLa cells stably expressing ATP10A. *A–D*, HeLa cells stably expressing HA-tagged P4-ATPase, as indicated, were established by infection with recombinant retrovirus and subsequent selection in the presence of G418. The cells were incubated with the indicated NBD-lipids at 15 °C for the indicated times. After extraction with fatty acid-free BSA, residual fluorescence intensity associated with cells was determined by flow cytometry. The fold increase in NBD-lipid uptake relative to that in vector-infected control cells (–) is shown. The graphs display averages from three independent experiments \pm S.D. (*, $p < 0.05$; **, $p < 0.01$). *E–H*, parental HeLa cells (*open squares*) or cells stably expressing ATP10A (*closed squares*) were incubated with indicated NBD-lipids at 15 °C for the indicated times (*x axis*). Graphs are representative of two independent experiments, and the results display averages from triplicates \pm S.D. *I*, HeLa cells stably expressing HA-tagged P4-ATPase were lysed and subjected to SDS-PAGE and immunoblotting using anti-HA or anti- β -tubulin antibody to determine the total expression level of the P4-ATPase protein. *J*, HeLa cells stably expressing HA-tagged ATP10A or ATP10A(E203Q) were treated with a pool of siRNA for LacZ or ATP10A. After 120 h, the cells were lysed and subjected to SDS-PAGE and immunoblotting using anti-HA or anti- β -tubulin antibody. *K–N*, cells treated with a pool of siRNAs targeting LacZ or ATP10A were incubated with the indicated NBD-lipids at 15 °C, as described in *A*. The fold increase in NBD-lipid uptake relative to vector-infected control cells is shown. Graphs display averages from three independent experiments \pm S.D. (*, $p < 0.05$; **, $p < 0.01$).

We also examined the time course of flippase activities in ATP10A-expressing cells (Fig. 3, *E–H*). HeLa cells stably expressing ATP10A exhibited a more dramatic increase in the amount of BSA-non-extractable NBD-PC than control HeLa cells (Fig. 3*E*). By contrast, the time-dependent increase in the amount of NBD-PS, NBD-PE, or NBD-SM in ATP10A-expressing cells did not differ significantly from that in control cells (Fig. 3, *F–H*). We did not detect flippase activity of ATP10D toward any of the NBD-lipids we examined. ATP10D might have flippase activity toward other lipids, although we cannot exclude a possibility that the flippase activity of ATP10D was undetectable due to its low specific activity and/or low expression level in the stable cells (Fig. 3*I*).

To confirm that the PC flipping activity observed in the ATP10A-expressing cells was indeed due to ATP10A expression, we treated cells stably expressing ATP10A or ATP10A(E203Q) with siRNAs targeting ATP10A and examined their flippase activities. Immunoblot analysis revealed that the expression level of ATP10A or ATP10A(E203Q) was significantly reduced in knockdown cells (Fig. 3*J*). In parallel

with the decrease in ATP10A expression levels, the flipping activity toward NBD-PC was dramatically decreased by treatment with ATP10A siRNA but not control siRNAs (siRNAs for LacZ) (Fig. 3*K*), indicating that the observed PC flipping activity could be attributed to ATP10A expression. By contrast, ATP10A depletion did not affect the uptake of other NBD-lipids (Fig. 3, *L–N*). Notably, depletion of ATP10A in control HeLa cells did not decrease basal PC flipping activity (Fig. 3*K*, *open* and *closed bars* in vector).

Co-expression of CDC50A, but Not CDC50B, with ATP10A or ATP11A Increases the Phospholipid Flipping Activities—Here and in our previous study, we showed that ATP10A, ATP8B1, and ATP11A are localized to the plasma membrane in a CDC50A-dependent manner. Therefore, we asked whether the phospholipid flipping activities of ATP10A, ATP8B1, and ATP11A are dependent on CDC50A as well. To this end, we transiently co-expressed ATP10A, ATP8B1, and ATP11A with either CDC50A or CDC50B in HeLa cells and subjected the cells to the flippase assay. Exogenous expression of ATP10A alone moderately increased flippase activity toward NBD-PC

ATP10A Translocates Phosphatidylcholine

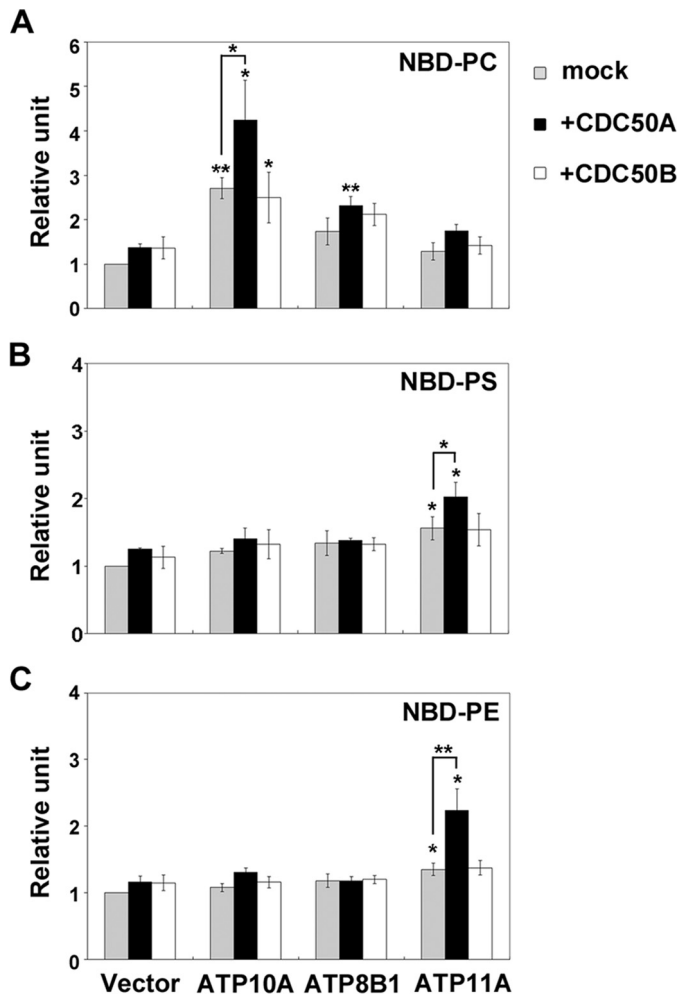


FIGURE 4. Co-expression of ATP10A with CDC50A, but not CDC50B, increases flippase activities. HeLa cells were transiently transfected with an expression vector encoding HA-tagged ATP10A, ATP8B1, or ATP11A either alone or together with a vector encoding FLAG-CDC50A or FLAG-CDC50B. After 48 h, cells were incubated with NBD-PC (A), NBD-PS (B), or NBD-PE (C) at 15 °C, and the residual fluorescence intensity associated with cells was determined by flow cytometry as described in the legend for Fig. 3. The fold increase in NBD-lipid uptake relative to vector-transfected HeLa cells is shown. Graphs display averages from three independent experiments \pm S.D. (*, $p < 0.05$; **, $p < 0.01$).

relative to vector-transfected control cells (Fig. 4A, gray bar), suggesting that some ATP10A might be transported to the plasma membrane by endogenous CDC50A. Co-expression of CDC50A with ATP10A further increased the PC flipping activity (Fig. 4A, closed bar). By contrast, cells co-expressing CDC50B with ATP10A (Fig. 4A, open bar) exhibited a PC flipping activity comparable to those expressing ATP10A alone (gray bar). Co-expression of ATP11A with CDC50A, but not CDC50B, increases flipping activity toward NBD-PS and NBD-PE (Fig. 4, B and C). These results are consistent with Figs. 1 and 2, showing that ATP10A and ATP11A are delivered to the plasma membrane in a CDC50A-dependent manner, and are thus able to exert flipping activity. Expression of ATP8B1 tended to increase PC flipping activity, although the effect was not statistically significant (Fig. 4A, gray bar), and co-expression of ATP8B1 with CDC50A slightly but significantly increased the activity (closed bar). The activity of ATP8B1 might be difficult to detect in transiently expressing cells,

because the PC flipping activity of ATP8B1 was much lower than that of ATP10A even in stably expressing cells (Fig. 3A).

CDC50A Knockdown Induces Mislocalization of ATP10A, ATP10D, ATP8B1, and ATP11A and Abolishes Flippase Activities—We next examined whether endogenous CDC50A is critical for plasma membrane localization and flippase activities of ATP10A, ATP10D, ATP8B1, and ATP11A. To this end, we knocked down endogenous CDC50A by RNAi in cells stably expressing ATP10A, ATP10D, ATP8B1 or ATP11A, and then examined whether CDC50A depletion affected their localization and flippase activities. Because no antibody against CDC50A was available, we confirmed specific and efficient knockdown of CDC50A by RT-PCR (Fig. 5F). As shown in Fig. 5A, CDC50A depletion caused mislocalization of ATP10A, ATP10D, ATP8B1, and ATP11A to the ER, overlapping with calnexin (Fig. 5, Ad, Ad', Ag, Ag', Aj, Aj', Am, and Am'). These observations strongly support the idea that endogenous CDC50A is required primarily for the ER exit and plasma membrane localization of ATP10A, ATP10D, ATP8B1, and ATP11A.

We next asked whether the flippase activities of cells stably expressing ATP10A, ATP8B1, or ATP11A were affected by CDC50A depletion. CDC50A depletion reversed the PC flipping activities observed in cells stably expressing ATP10A or ATP8B1 (Fig. 5B) and decreased the PS and PE flipping activities observed in ATP11A-expressing cells (Fig. 5, C and D). These data indicate that these P4-ATPases cannot be transported to the plasma membrane in the absence of CDC50A, abrogating the phospholipid flipping activities observed in cells stably expressing the P4-ATPases.

Notably, in vector-infected control HeLa cells, depletion of CDC50A markedly decreased PS and PE flipping activities, but barely decreased PC flipping activity (Fig. 5, B–D, open bars in vector). The dramatic decrease in PS flipping activities in cells depleted of CDC50A might be ascribed to failed delivery of endogenous PS-flipping P4-ATPases to the plasma membrane in the absence of CDC50A. These data are compatible with the fact that endogenous PS flipping activity in HeLa cells is much higher than the activities toward other phospholipids (compare Fig. 3, E–H, and also see Ref. 19). Therefore, the high and constitutive PS flipping activities might be required in HeLa cells to prevent the exposure of PS to the outer leaflet and to maintain the asymmetry between the two leaflets of the plasma membrane. On the other hand, the PC flipping event might occur at a very low rate at steady state, or it might be required under specific conditions (such as in response to signals) or in a specific place (such as the bile canaliculi) (19, 20, 34).

Enhanced PC Flipping Activity Alters Cell Shape and Decreases Cell Size—During the course of our experiments, we noticed that cell shape was significantly altered by overexpression of ATP10A but not the ATP10A(E203Q) mutant (Fig. 1, Ab, D, and F, and Fig. 6). As shown in Fig. 6A, the shape of cells transiently expressing ATP10A(WT) and CDC50A (Fig. 6Ac) was dramatically altered relative to that of control cells (Aa). By contrast, cells transiently expressing CDC50A alone (Fig. 6Ab) or those expressing ATP10A(E203Q) and CDC50A (Ad) did not exhibit an observable shape change relative to control cells (Aa). To quantitatively show the change in cell shape, we stained the cells with a plasma membrane marker, MHCI, and

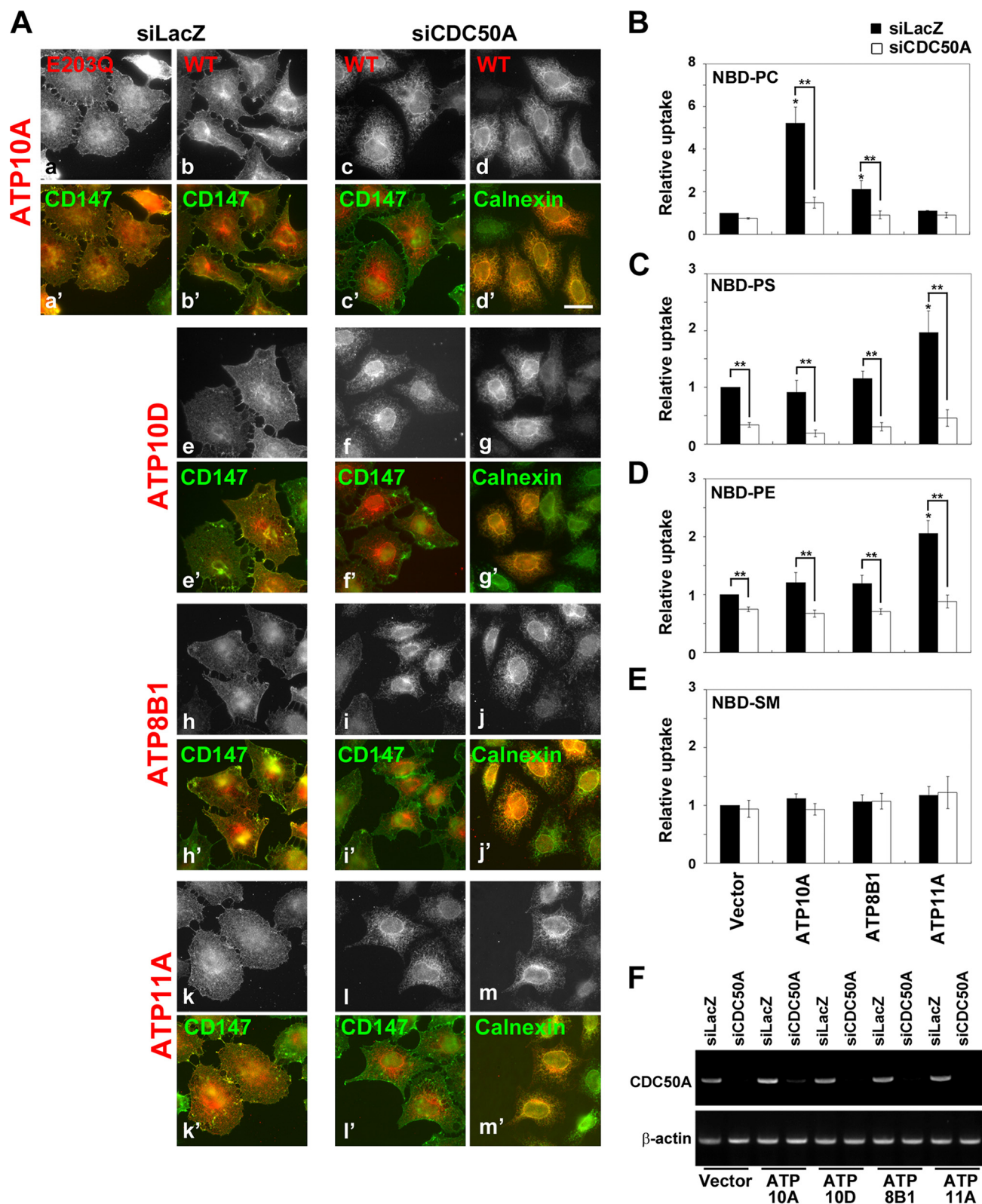


FIGURE 5. Depletion of CDC50A abolishes the plasma membrane localization of P4-ATPases and their flippase activities. *A*, HeLa cells stably expressing HA-tagged ATP10A, ATP10D, ATP8B1, or ATP11A were treated with a pool of siRNAs targeting LacZ or CDC50A. After 72 h, cells were fixed and processed for immunofluorescence analysis. For ER staining, the fixed and permeabilized cells were incubated with anti-HA and anti-calnexin antibodies followed by Cy3-conjugated anti-rat and Alexa Fluor 488-conjugated anti-mouse antibodies. For plasma membrane staining, cells were incubated with Alexa Fluor 488-conjugated anti-CD147 antibody prior to permeabilization and with anti-HA antibody after permeabilization, as described in the legend for Fig. 1, *D* and *F*. Bar, 20 μ m. *B–E*, siRNA-treated cells were incubated with the indicated NBD-lipids at 15 $^{\circ}$ C, and the residual fluorescence intensity associated with the cells was determined by flow cytometry as described in the legend for Fig. 3. The fold increase in NBD-lipid uptake compared with vector-infected and siLacZ-treated control cells is shown. Graphs display averages from three independent experiments \pm S.D. (*, $p < 0.05$; **, $p < 0.01$). *F*, siRNA-treated cells were lysed to isolate total RNAs, which were processed for RT-PCR.

ATP10A Translocates Phosphatidylcholine

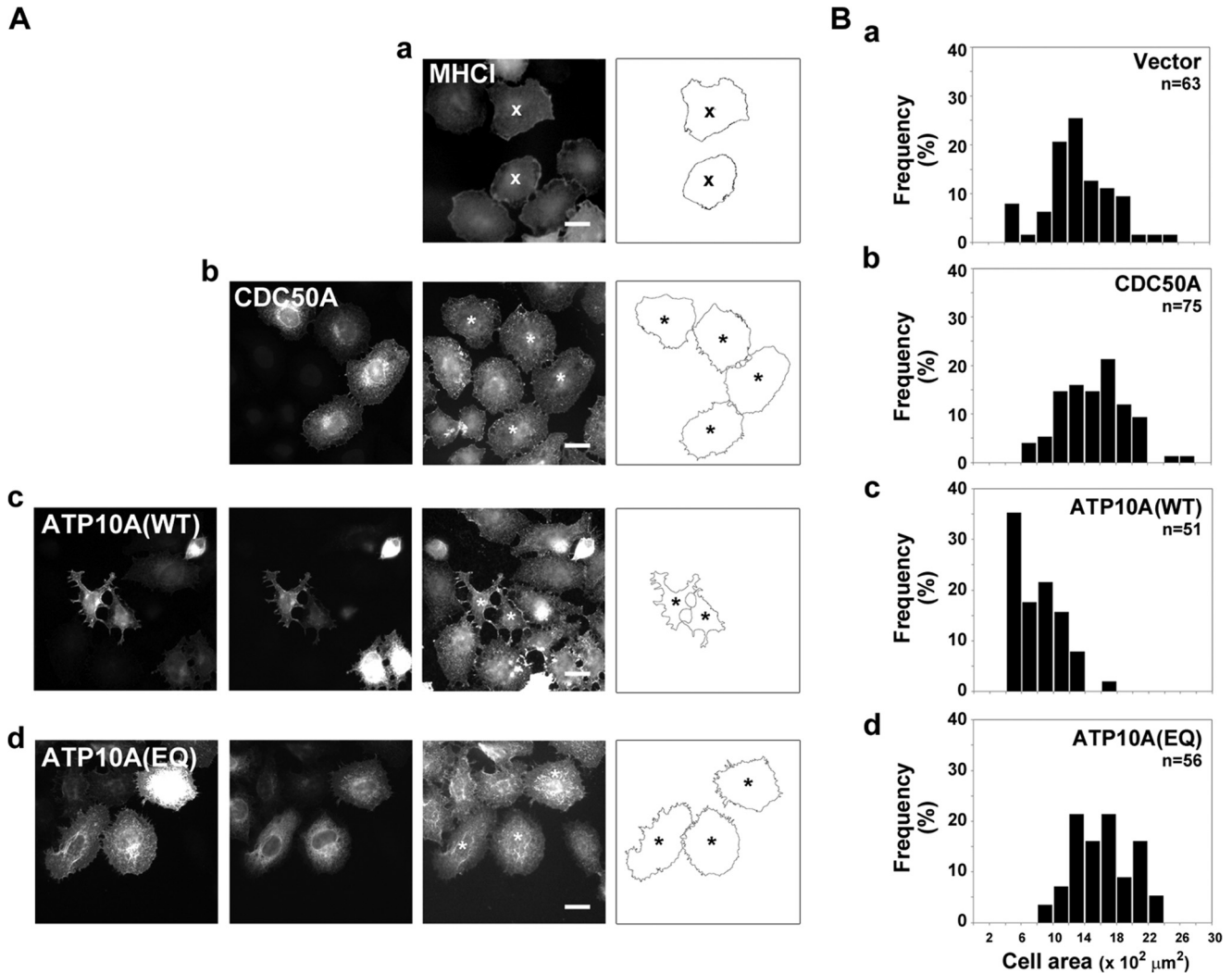


FIGURE 6. Overexpression of ATP10A causes a change in cell shape and a decrease in cell size. HeLa cells were transiently transfected with an empty expression vector (*a* panels) or an expression vector for FLAG-CDC50A (*b* panels) either alone or in combination with expression vector for ATP10A-HA (*c* panels) or ATP10A(E203Q)-HA (*d* panels). *A*, after 48 h, the cells were incubated with anti-MHCI antibody prior to fixation to label the cell surfaces. After fixation and permeabilization, the cells were incubated with anti-HA and anti-FLAG followed by Cy3-conjugated anti-rat, Alexa Fluor 488-conjugated anti-mouse, and Alexa Fluor 647-conjugated anti-rabbit antibodies. Bars, 20 μm . HeLa cells (*a*, cross marks) or cells expressing FLAG-CDC50A (*b*) or either ATP10A-HA (*c*) or ATP10A(E203Q)-HA (*d*) with FLAG-CDC50A (asterisks) were outlined by setting a threshold for the fluorescence intensities of MHC1 staining. *B*, each cell area was measured by ImageJ software, and the frequency distribution of the cell size is shown.

quantitated cell areas using the ImageJ software (Fig. 6, *A* and *B*). The frequency distribution of cell areas revealed that the population of small-sized cells markedly increased upon co-expression of ATP10A and CDC50A (Fig. 6*Bc*). By contrast, the frequency distribution of cell areas in cells co-expressing ATP10A(E203Q) and CDC50A (Fig. 6*Bd*) was not significantly changed relative to control (*Ba*) or CDC50A-expressing cells (*Bb*). These results indicate that the change in cell shape and decrease in cell size could be ascribed to enhanced PC flipping activity due to elevated expression of ATP10A at the plasma membrane.

Enhanced PC Flipping Activity Inhibits Cell Adhesion and Spreading—We next asked whether cell adhesion and spreading were altered by ATP10A expression. For this purpose, we examined the efficiency of cell adhesion in cells stably expressing ATP10A and ATP10A(E203Q). Cells detached from the dishes by treatment with EDTA were resuspended with medium supplemented with FBS and seeded onto plastic

dishes. After incubation for the indicated times, non-adherent cells were removed by washing with PBS, and adherent cells were stained with crystal violet. The stain was then extracted from cells and quantitated by measuring the absorbance at 570 nm; although the same numbers of cells were seeded, the absorbance was normalized to the DNA content of the seeded cells to achieve a more accurate assessment. As shown in Fig. 7, *A* and *B*, adhesion of ATP10A-expressing cells was delayed relative to the control cells. By contrast, adhesion of ATP10A(E203Q)-expressing cells was not delayed but instead was slightly accelerated. After 60 min of incubation, cell adhesion was comparable among cells expressing ATP10A or ATP10A(E203Q) and control cells (Fig. 7*A*). Thus, cell adhesion was delayed in cells expressing ATP10A(WT). Notably, the extent of cell spreading at the 60-min time point appeared to be lower in cells expressing ATP10A(WT) (Fig. 7*B*, middle panel) relative to control and ATP10A(E203Q)-expressing cells (Fig. 7*B*, top and bottom panels, respectively). Therefore, we next asked whether cell

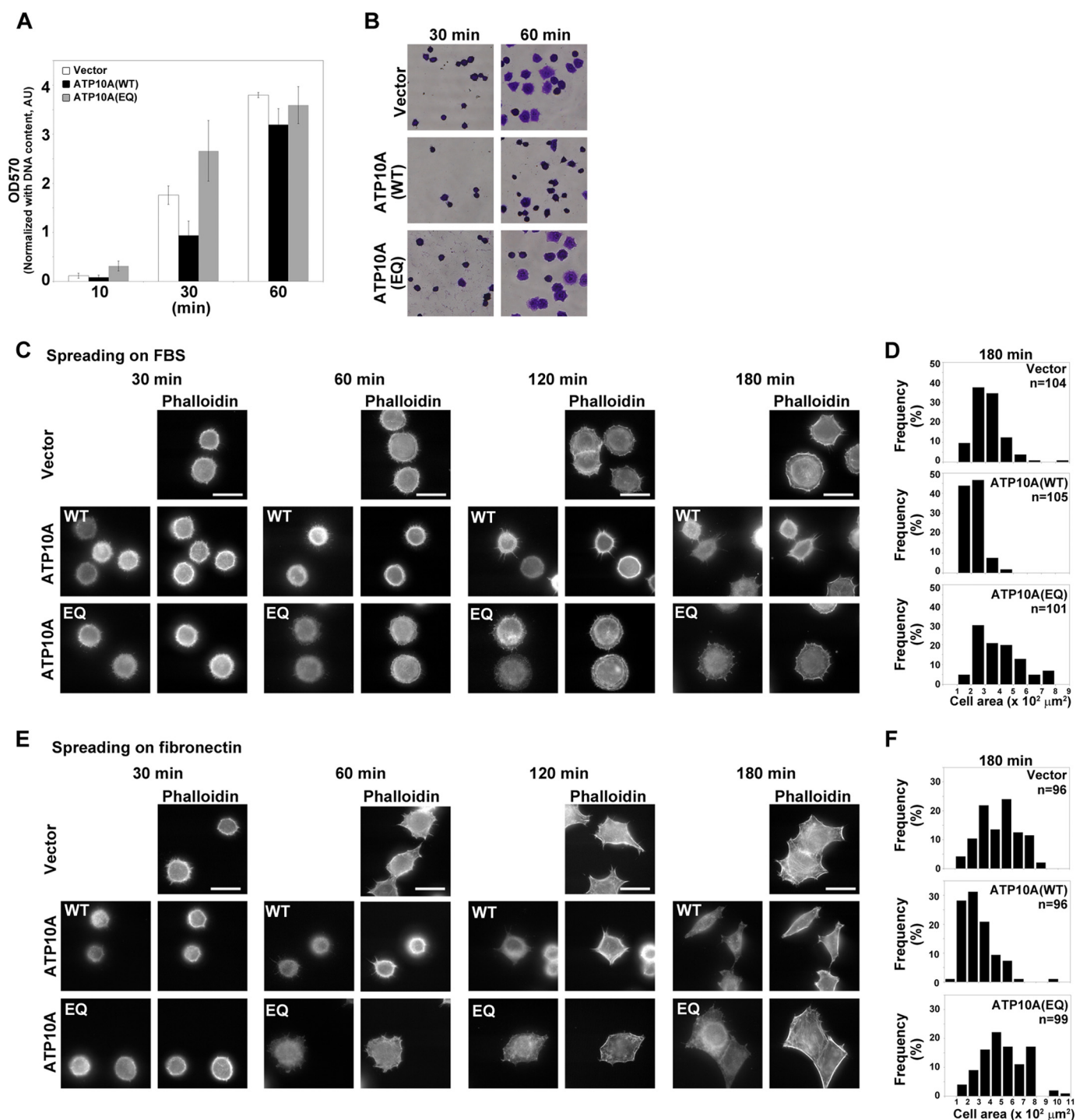


FIGURE 7. Enhanced PC flipping activity delays cell adhesion and spreading. *A* and *B*, adhesion assay was performed using HeLa cells stably expressing ATP10A-HA or ATP10A(E203Q)-HA. Cells were seeded onto a plastic dish and incubated for the indicated times. After washing to remove non-adherent cells, adherent cells were fixed and stained with crystal violet. The stain was processed for measurement of absorbance at 570 nm. In *B*, representative images of cells stained with crystal violet are shown. *C–F*, HeLa cells stably expressing ATP10A-HA or ATP10A(E203Q)-HA were processed for the spreading assay. Cells were seeded onto FBS (*C* and *D*)- or fibronectin (*E* and *F*)-coated coverslips and incubated for the indicated times. After fixation and permeabilization, cells were incubated with anti-HA antibody followed by Cy3-conjugated anti-rat antibody and Alexa Fluor 488-conjugated phalloidin (*C* and *E*). Bars, 20 μm . *D* and *F*, cell areas were measured by the MetaMorph software, and the frequency distribution of cell areas at 180 min is shown.

spreading was affected by expression of ATP10A. To this end, cells stably expressing ATP10A(WT) or ATP10A(E203Q) were detached from dishes by EDTA treatment, resuspended in serum-free medium, and seeded onto FBS- or fibronectin-coated coverslips. As shown in Fig. 7, *C* and *E*, cells stably expressing ATP10A spread more slowly onto the FBS- or fibronectin-coated coverslips

than control cells and those expressing ATP10A(E203Q) (compare the cells at 60-, 120-, and 180-min time points). We quantitated the areas of the cells at the 180-min time point using MetaMorph software (Fig. 7, *D* and *F*). The frequency distribution of cell areas revealed that the population of small-sized cells increased significantly upon stable expression of ATP10A(WT) but not

ATP10A Translocates Phosphatidylcholine

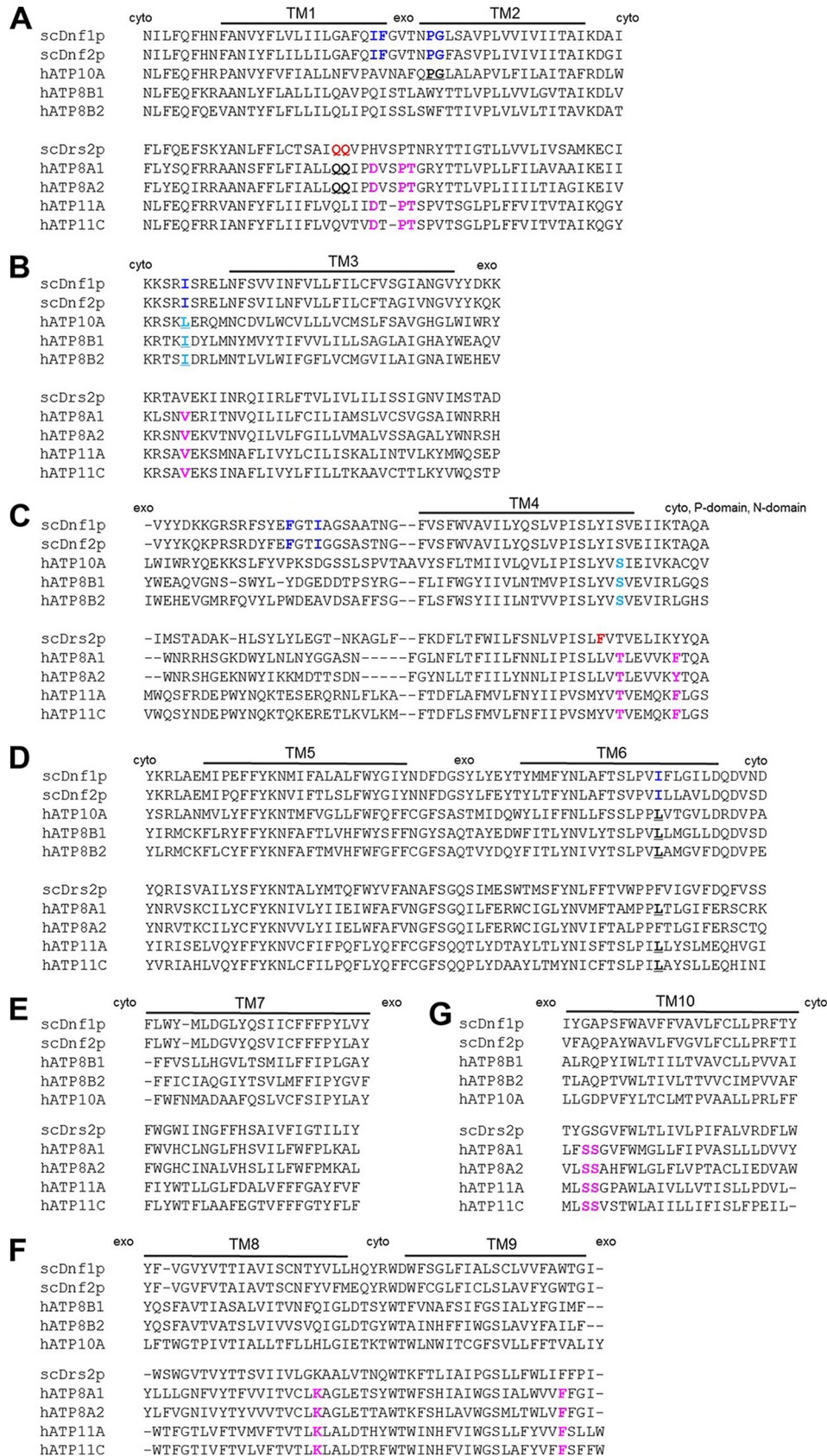


FIGURE 8. Sequence alignment of PC- and PS-flipping P4-ATPases. A–C, the upper and lower panels show PC- and PS-flipping P4-ATPases, respectively. A–G, alignment of putative amino acid sequences of TM1–2 (A), TM3 (B), exoplasmic region between TM3 and TM4–TM4 (C), TM5–6 (D), TM7 (E), TM8–9 (F), and TM10 (G). Bold blue letters are putative residues for PC specificity, and bold red letters are putative residues for PS specificity (36). Bold underlined letters show the conserved residues with the blue or red amino acids. Bold light blue letters and bold pink letters represent residues conserved among mammalian PC-flippases and PS-flippases, respectively. *exo*, exoplasmic; *cyto*, cytoplasmic; *P-domain*, phosphorylation domain; *N-domain*, nucleotide-binding domain.

ATP10A(E203Q) (Fig. 7, *D* and *F*). Taken together, these observations indicate that the suppression of cell adhesion and cell spreading observed in cells expressing ATP10A can be ascribed to enhanced PC flipping activity.

Discussion

In this study, we demonstrated that class 5 P4-ATPases (ATP10A, ATP10B, and ATP10D) require interaction with CDC50A for their exit from the ER and localization to specific cellular compartments where they exert their functions (Fig. 1). Importantly, we revealed that ATP10A has PC-specific flipping activity. Moreover, the enhanced PC flipping activity resulting from expression of ATP10A leads to changes in cell shape and delays cell adhesion and spreading.

Unlike ATP8B1 and ATP11A, members of the ATP10 family (especially ATP10B and ATP10D) associate with glycosylated CDC50A with low affinity (Fig. 2). Even if the interaction between ATP10 proteins and CDC50A is not as strong as that between ATP8B1 or ATP11A and CDC50A, the interaction is nonetheless critical for the localization of ATP10 proteins to their final destinations: the plasma membrane for ATP10A and ATP10D and late endosomes for ATP10B (Fig. 1). In support of this result, these P4-ATPases did not exit the ER in cells depleted of CDC50A (Fig. 5A). By contrast, CDC50B was dispensable for the exit of ATP10 proteins from the ER.

Importantly, exogenous expression of ATP10A in HeLa cells dramatically increases NBD-PC flipping activity but not flipping of NBD-aminophospholipids (Fig. 3). This activity was abolished by treatment with siCDC50A, confirming that CDC50A is critical for plasma membrane localization of ATP10A (Fig. 5). We did not detect any flippase activity of ATP10D toward PC, PS, PE, or SM. However, ATP10D may have flippase activities toward other phospholipids that were not tested in this study or may exhibit activity in response to specific signaling events.

In yeast, Dnf1p prefers PC and PE (9, 35), whereas Drs2p prefers PS (11). Several key residues have been proposed to determine the phospholipid specificities of Drs2p and Dnf1p (36, 37). We aligned and compared the primary sequences between the PS- and PC-flipping P4-ATPases in yeast and human (Fig. 8) (19, 38). Many of the key residues required for the PC flipping activity of Dnf1p are not conserved in PC-flipping human P4-ATPases (ATP10A, ATP8B1, and ATP8B2) except for the Ile residue, located in the cytoplasmic region close to the TM3 (Fig. 8*B*, **bold blue letters** and underlined bold letters). Some residues required for PS selectivity of Drs2p (Fig. 8*B*, **bold red letters**) (36) are not conserved in PS-flipping human P4-ATPases. Thus, the residues that contribute to PC and PS selectivity in yeast P4-ATPases do not always hold true for human P4-ATPases. On the other hand, some residues are conserved among mammalian PC-specific P4-ATPases (Fig. 8, **bold light blue letters**), and others are conserved among PS-specific P4-ATPases (**bold pink letters**), raising an interesting question of whether these residues are critical for determining substrate specificities.

The increase in PC flipping activity resulting from ATP10A expression may alter the plasma membrane dynamics, resulting in drastic changes in cell shape and a reduction in cell size.

Moreover, cell adhesion and spreading onto the extracellular matrix were significantly delayed by ATP10A expression. By contrast, expression of ATP10A(E203Q), an ATPase-deficient mutant, affected neither the cell shape nor cell spreading, indicating that these phenotypic changes caused by ATP10A expression can be ascribed to enhanced PC flipping activity at the plasma membrane. Although the exact molecular mechanism underlying the phenotypic changes induced by ATP10A expression remains to be addressed in future studies, we propose two hypotheses: 1) Because PC is the most abundant phospholipid in cellular membranes, enhanced translocation of PC from the extracellular to the cytoplasmic leaflet increases the PC ratio of the cytoplasmic leaflet to the extracellular leaflet, favoring positive curvature toward the cytoplasm. Therefore, outward growth of cells, such as cell spreading, might be inhibited, resulting in a reduction in cell size. Compatible with this possibility, a mutation in mouse ATP11C, which flips PS and PE at the plasma membrane, alters erythrocyte morphology (24). 2) The enhanced translocation of PC to the cytoplasmic leaflet may reduce the local concentration of PS or phosphatidylinositol 4,5-bisphosphate (PIP₂) in the cytoplasmic leaflet. Because PS and PIP₂ play critical roles in remodeling of the actin cytoskeleton for cell adhesion, spreading, and migration, a decrease in the local concentration of PS or PIP₂ might inhibit cell adhesion and spreading. Indeed, in budding yeast, local concentration of PS is indispensable for recruitment of Cdc42 to polarized bud tips, and both PS concentration and Cdc42 recycling are regulated by the flippase activity of Dnf1p/Dnf2p, which flips PE and PC (39, 40).

Genetic studies demonstrate that Dnf1p/Dnf2p translocate lyso-PE and lyso-PC into the inner/cytoplasmic leaflet of the plasma membrane, and they are in turn converted to PE and PC, respectively, by an acyltransferase. Therefore, lyso-PE and lyso-PC might be sources for the synthesis of PE and PC to support the lipid content and membrane biogenesis in yeast (41). Hence, we cannot exclude the possibility that ATP10A might be able to transport lyso-PC.

Depletion of CDC50A dramatically decreased the PS flipping activity but did not significantly decrease the PC flipping activity in HeLa cells. Therefore, it is likely that the basal PC flipping activity by endogenous P4-ATPases in HeLa cells is not as high as the PS flipping activity, which is indispensable for preventing unnecessary exposure of PS to the exoplasmic leaflet of the plasma membrane. A recent study showed that knock-out of CDC50A in KBM-7 cells dramatically decreases flipping activity toward PC as well as PS (25). In addition, the PC flipping activity of ATP8B1 is required for proper bile excretion in the liver (19, 34, 42). Therefore, the level of basal PC flipping activity might vary in different cell types and tissues, raising questions about the regulation of PC flipping activity. In budding yeast, the P4-ATPases (preferentially Dnf1p and Dnf2p) require phosphorylation by Fpk1 for their functions (43), and Drs2p requires an interaction with phosphatidylinositol 4-phosphate for its activity (44). It is tempting to speculate that PC-flipping P4-ATPases might be regulated by phosphorylation in response to specific cellular signaling events or by their interactions with specific regulatory factors.

References

- Op den Kamp, J. A. (1979) Lipid asymmetry in membranes. *Annu. Rev. Biochem.* **48**, 47–71
- van Meer, G., Voelker, D. R., and Feigenson, G. W. (2008) Membrane lipids: where they are and how they behave. *Nat. Rev. Mol. Cell Biol.* **9**, 112–124
- Leventis, P. A., and Grinstein, S. (2010) The distribution and function of phosphatidylserine in cellular membranes. *Annu. Rev. Biophys.* **39**, 407–427
- Schrier, S. L., Zachowski, A., and Devaux, P. F. (1992) Mechanisms of amphipath-induced stomatocytosis in human erythrocytes. *Blood* **79**, 782–786
- Zwaal, R. F., and Schroit, A. J. (1997) Pathophysiologic implications of membrane phospholipid asymmetry in blood cells. *Blood* **89**, 1121–1132
- Seigneuret, M., and Devaux, P. F. (1984) ATP-dependent asymmetric distribution of spin-labeled phospholipids in the erythrocyte membrane: relation to shape changes. *Proc. Natl. Acad. Sci. U.S.A.* **81**, 3751–3755
- Tang, X., Halleck, M. S., Schlegel, R. A., and Williamson, P. (1996) A subfamily of P-type ATPases with aminophospholipid transporting activity. *Science* **272**, 1495–1497
- Daleke, D. L. (2003) Regulation of transbilayer plasma membrane phospholipid asymmetry. *J. Lipid Res.* **44**, 233–242
- Pomorski, T., Lombardi, R., Riezman, H., Devaux, P. F., van Meer, G., and Holthuis, J. C. (2003) Drs2p-related P-type ATPases Dnf1p and Dnf2p Are Required for Phospholipid Translocation across the Yeast Plasma Membrane and Serve a Role in Endocytosis. *Mol. Biol. Cell* **14**, 1240–1254
- Saito, K., Fujimura-Kamada, K., Furuta, N., Kato, U., Umeda, M., and Tanaka, K. (2004) Cdc50p, a protein required for polarized growth, associates with the Drs2p P-type ATPase implicated in phospholipid translocation in *Saccharomyces cerevisiae*. *Mol. Biol. Cell* **15**, 3418–3432
- Zhou, X., and Graham, T. R. (2009) Reconstitution of phospholipid translocase activity with purified Drs2p, a type-IV P-type ATPase from budding yeast. *Proc. Natl. Acad. Sci. U.S.A.* **106**, 16586–16591
- Natarajan, P., Wang, J., Hua, Z., and Graham, T. R. (2004) Drs2p-coupled aminophospholipid translocase activity in yeast Golgi membranes and relationship to *in vivo* function. *Proc. Natl. Acad. Sci. U.S.A.* **101**, 10614–10619
- Furuta, N., Fujimura-Kamada, K., Saito, K., Yamamoto, T., and Tanaka, K. (2007) Endocytic Recycling in yeast is regulated by putative phospholipid translocases and the Ypt31p/32p-Rcy1p pathway. *Mol. Biol. Cell* **18**, 295–312
- Paulusma, C. C., Folmer, D. E., Ho-Mok, K. S., de Waart, D. R., Hilarius, P. M., Verhoeven, A. J., and Oude Elferink, R. P. (2008) ATP8B1 requires an accessory protein for endoplasmic reticulum exit and plasma membrane lipid flippase activity. *Hepatology* **47**, 268–278
- Bryde, S., Hennrich, H., Verhulst, P. M., Devaux, P. F., Lenoir, G., and Holthuis, J. C. (2010) CDC50 proteins are critical components of the human class-1 P4-ATPase transport machinery. *J. Biol. Chem.* **285**, 40562–40572
- van der Velden, L. M., Wichers, C. G., van Breevoort, A. E., Coleman, J. A., Molday, R. S., Berger, R., Klomp, L. W., and van de Graaf, S. F. (2010) Heteromeric interactions required for abundance and subcellular localization of human CDC50 proteins and class 1 P4-ATPases. *J. Biol. Chem.* **285**, 40088–40096
- Coleman, J. A., and Molday, R. S. (2011) Critical Role of the b-subunit CDC50A in the stable expression, assembly, subcellular localization, and lipid transport activity of the P4-ATPase ATP8A2. *J. Biol. Chem.* **286**, 17205–17216
- Takatsu, H., Baba, K., Shima, T., Umino, H., Kato, U., Umeda, M., Nakayama, K., and Shin, H. W. (2011) ATP9B, a P4-ATPase (a putative aminophospholipid translocase), localizes to the trans-Golgi network in a CDC50 protein-independent manner. *J. Biol. Chem.* **286**, 38159–38167
- Takatsu, H., Tanaka, G., Segawa, K., Suzuki, J., Nagata, S., Nakayama, K., and Shin, H. W. (2014) Phospholipid flippase activities and substrate specificities of human type IV P-type ATPases localized to the plasma membrane. *J. Biol. Chem.* **289**, 33543–33556
- Paulusma, C. C., Groen, A., Kunne, C., Ho-Mok, K. S., Spijkerboer, A. L., Rudi de Waart, D., Hoek, F. J., Vreeling, H., Hoeben, K. A., van Marle, J., Pawlikowska, L., Bull, L. N., Hofmann, A. F., Knisely, A. S., and Oude Elferink, R. P. (2006) Atp8b1 deficiency in mice reduces resistance of the canalicular membrane to hydrophobic bile salts and impairs bile salt transport. *Hepatology* **44**, 195–204
- Folmer, D. E., Elferink, R. P., and Paulusma, C. C. (2009) P4 ATPases-lipid flippases and their role in disease. *Biochim. Biophys. Acta* **1791**, 628–635
- Levano, K., Punia, V., Raghunath, M., Debata, P. R., Curcio, G. M., Mogha, A., Purkayastha, S., McCloskey, D., Fata, J., and Banerjee, P. (2012) Atp8a1 deficiency is associated with phosphatidylserine externalization in hippocampus and delayed hippocampus-dependent learning. *J. Neurochem.* **120**, 302–313
- Yabas, M., Teh, C. E., Frankenreiter, S., Lal, D., Roots, C. M., Whittle, B., Andrews, D. T., Zhang, Y., Teoh, N. C., Sprent, J., Tze, L. E., Kucharska, E. M., Kofler, J., Farrell, G. C., Bröer, S., Goodnow, C. C., and Enders, A. (2011) ATP11C is critical for the internalization of phosphatidylserine and differentiation of B lymphocytes. *Nat. Immunol.* **12**, 441–449
- Yabas, M., Coupland, L. A., Cromer, D., Winterberg, M., Teoh, N. C., D’Rozario, J., Kirk, K., Bröer, S., Parish, C. R., and Enders, A. (2014) Mice deficient in the putative phospholipid flippase ATP11C eXHIBIT altered erythrocyte shape, anemia, and reduced erythrocyte life span. *J. Biol. Chem.* **289**, 19531–19537
- Segawa, K., Kurata, S., Yanagihashi, Y., Brummelkamp, T. R., Matsuda, F., and Nagata, S. (2014) Caspase-mediated cleavage of phospholipid flippase for apoptotic phosphatidylserine exposure. *Science* **344**, 1164–1168
- Dhar, M. S., Sommardahl, C. S., Kirkland, T., Nelson, S., Donnell, R., Johnson, D. K., and Castellani, L. W. (2004) Mice heterozygous for Atp10c, a putative amphipath, represent a novel model of obesity and type 2 diabetes. *J. Nutr.* **134**, 799–805
- Hurst, S. E., Minkin, S. C., Biggerstaff, J., and Dhar, M. S. (2012) Transient silencing of a type IV P-type ATPase, Atp10c, results in decreased glucose uptake in C2C12 myotubes. *J. Nutr. Metab.* **2012**, 152902
- Dhar, M. S., Yuan, J. S., Elliott, S. B., and Sommardahl, C. (2006) A type IV P-type ATPase affects insulin-mediated glucose uptake in adipose tissue and skeletal muscle in mice. *J. Nutr. Biochem.* **17**, 811–820
- Yamamoto, H., Koga, H., Katoh, Y., Takahashi, S., Nakayama, K., and Shin, H. W. (2010) Functional cross-talk between Rab14 and Rab4 through a dual effector, RUFY1/Rabip4. *Mol. Biol. Cell* **21**, 2746–2755
- Shin, H. W., Kobayashi, H., Kitamura, M., Waguri, S., Sugauma, T., Uchiyama, Y., and Nakayama, K. (2005) Roles of ARFRP1 (ADP-ribosylation factor-related protein 1) in post-Golgi membrane trafficking. *J. Cell Sci.* **118**, 4039–4048
- Shin, H. W., Morinaga, N., Noda, M., and Nakayama, K. (2004) BIG2, a Guanine Nucleotide Exchange Factor for ADP-Ribosylation Factors: Its Localization to Recycling Endosomes and Implication in the Endosome Integrity. *Mol. Biol. Cell* **15**, 5283–5294
- Anthonisen, A. N., Clausen, J. D., and Andersen, J. P. (2006) Mutational analysis of the conserved TGES loop of sarcoplasmic reticulum Ca²⁺-ATPase. *J. Biol. Chem.* **281**, 31572–31582
- Morita, S. Y., Kobayashi, A., Takanezawa, Y., Kioka, N., Handa, T., Arai, H., Matsuo, M., and Ueda, K. (2007) Bile salt-dependent efflux of cellular phospholipids mediated by ATP-binding cassette protein B4. *Hepatology* **46**, 188–199
- Folmer, D. E., van der Mark, V. A., Ho-Mok, K. S., Oude Elferink, R. P., and Paulusma, C. C. (2009) Differential effects of progressive familial intrahepatic cholestasis type 1 and benign recurrent intrahepatic cholestasis type 1 mutations on canalicular localization of ATP8B1. *Hepatology* **50**, 1597–1605
- Kato, U., Emoto, K., Fredriksson, C., Nakamura, H., Ohta, A., Kobayashi, T., Murakami-Murofushi, K., Kobayashi, T., and Umeda, M. (2002) A novel membrane protein, Ros3p, is required for phospholipid translocation across the plasma membrane in *Saccharomyces cerevisiae*. *J. Biol. Chem.* **277**, 37855–37862
- Baldrige, R. D., and Graham, T. R. (2013) Two-gate mechanism for phospholipid selection and transport by type IV P-type ATPases. *Proc. Natl. Acad. Sci. U.S.A.* **110**, E358–E367
- Baldrige, R. D., and Graham, T. R. (2012) Identification of residues de-

- fining phospholipid flippase substrate specificity of type IV P-type ATPases. *Proc. Natl. Acad. Sci. U.S.A.* **109**, E290–E298
38. Lee, S., Uchida, Y., Wang, J., Matsudaira, T., Nakagawa, T., Kishimoto, T., Mukai, K., Inaba, T., Kobayashi, T., Molday, R. S., Taguchi, T., and Arai, H. (2015) Transport through recycling endosomes requires EHD1 recruitment by a phosphatidylserine translocase. *EMBO J.* **34**, 669–688
 39. Fairn, G. D., Hermansson, M., Somerharju, P., and Grinstein, S. (2011) Phosphatidylserine is polarized and required for proper Cdc42 localization and for development of cell polarity. *Nat. Cell Biol.* **13**, 1424–1430
 40. Das, A., Slaughter, B. D., Unruh, J. R., Bradford, W. D., Alexander, R., Rubinstein, B., and Li, R. (2012) Flippase-mediated phospholipid asymmetry promotes fast Cdc42 recycling in dynamic maintenance of cell polarity. *Nat. Cell Biol.* **14**, 304–310
 41. Riekhof, W. R., and Voelker, D. R. (2009) The yeast plasma membrane P4-ATPases are major transporters for lysophospholipids. *Biochim. Biophys. Acta* **1791**, 620–627
 42. Klomp, L. W., Vargas, J. C., van Mil, S. W., Pawlikowska, L., Strautnieks, S. S., van Eijk, M. J., Juijn, J. A., Pabón-Peña, C., Smith, L. B., DeYoung, J. A., Byrne, J. A., Gombert, J., van der Brugge, G., Berger, R., Jankowska, I., Pawlowska, J., Villa, E., Knisely, A. S., Thompson, R. J., Freimer, N. B., Houwen, R. H., and Bull, L. N. (2004) Characterization of mutations in ATP8B1 associated with hereditary cholestasis. *Hepatology* **40**, 27–38
 43. Nakano, K., Yamamoto, T., Kishimoto, T., Noji, T., and Tanaka, K. (2008) Protein kinases Fpk1p and Fpk2p are novel regulators of phospholipid asymmetry. *Mol. Biol. Cell* **19**, 1783–1797
 44. Natarajan, P., Liu, K., Patil, D. V., Sciorra, V. A., Jackson, C. L., and Graham, T. R. (2009) Regulation of a Golgi flippase by phosphoinositides and an ArpGEF. *Nat. Cell Biol.* **11**, 1421–1426